Int. J. Heat Mass Transfer. Vol. 33, No. 4, pp. 611–620, 1990
Printed in Great Britain

0017–9310/90 $3.00+0.00

A physical approach to critical heat flux of subcooled flow boiling in round tubes

Y. KATTO

Department of Mechanical Engineering, Nihon University, Kanda-Surugadai, Chiyoda-ku, Tokyo 101, Japan

(*Received* 24 *January* 1989)

Abstract—This paper presents an analysis of the critical heat flux (CHF) of subcooled flow boiling based on the liquid sublayer dryout mechanism, assuming that it is a similar phenomenon to CHF in pool boiling except for apparent differences between forced and natural convection. Employing the same formula of sublayer thickness as that derived for CHF in pool boiling, a physcial model of CHF is derived with an empirical coefficient relating to the velocity of a vapor blanket sliding on a thin liquid sublayer. Predicted CHF values are compared with experimental data for water, R-12, R-11, nitrogen, helium, and R-113, respectively, suggesting propriety of the present model.

1. INTRODUCTION

FOR THE critical heat flux (CHF) of subcooled or low quality flow boiling, various models have so far been considered in its analytical or data correlation studies. Roughly speaking, however, they may be classified into five groups which can be arranged in the following chronological order.

(1) Liquid layer superheat limit model (1965). Tong *et al.* [1] assume that CHF occurs when the liquid layer adjacent to the wall has a critical superheat caused by the difficulty of enthalpy transport across the overlying bubbly layer.

(2) Boundary layer separation model (1968–1975). The studies of Kutateladze and Leont'ev [2], Tong [3, 4], Purcupile and Gouse [5], and Hancox and Nicoll [6] are associated with this model, where flow stagnation due to injection of vapor from the wall is assumed to originate CHF. Though it has a different appearance, the model of Thorgerson *et al.* [7] also may be regarded as a peculiar modification of this group, because of paying attention to the role of the friction factor.

(3) Liquid flow blockage model (1980–1981). This model postulates that CHF occurs when the liquid flow normal to the wall is blocked by the flow of vapor. There are two versions: Bergel'son [8] considers a critical velocity raised by the instability of the vapor–liquid interface, while Smogalev [9] considers the effect of the kinetic energy of vapor flow overcoming the counter motion of liquid.

(4) Vapor removal limit and bubble crowding model (1981–1985). Hebel *et al.* [10] assume that limitation for the rate of the vapor removal by axial transport of vapor bubbles leads to the shortage of liquid, that is, CHF. Weisman and co-workers [11, 12] consider a critical value of void fraction in the bubble layer adjacent to the wall, which is brought about through the balance between the outward flow of vapor bubbles and the inward flow of liquid at the bubble-layer/bulk-flow interface. Their CHF model made with two empirical constants gives good predictions for various kinds of fluids under slightly subcooled and low quality conditions. The model of Yagov and Puzin [13] may be regarded as a special species belonging to this group.

(5) Liquid sublayer dryout model (1988). The recent study by Lee and Mudawar [14] presents a model postulating the onset of CHF due to the dryout of a thin liquid sublayer underneath a vapor blanket flowing over the wall. Their model made with a constant and a coefficient, both determined empirically, can predict CHF of water fairly well over a considerably wide range of subcooling.

Meanwhile, existing experimental studies have revealed the following phenomena associated with CHF in subcooled or low quality flow boiling.

(1) Existence of vapor slugs or thin vapor layers near the wall. Through photography or other means, Tong *et al.* [15], Fiori and Bergles [16], Molen and Galjee [17], and Hino and Ueda [18] observed the liquid–vapor flow configuration near CHF for water at 0.1–0.2 MPa and R-113 at 0.1–0.36 MPa. Their results, associated with comparatively low pressure systems, show the appearance of vapor slugs near the wall. Meanwhile, Mattson *et al.* [19] performed an experiment for R-113 at higher pressures of 0.69–2.4 MPa, which suggests that vapor bubbles are small in high pressure systems, but thin vapor layers are observed on the wall at CHF.

(2) Fluctuant phenomena observed prior to CHF. Fiori and Bergles [16] have reported the observation of the wall temperature fluctuation prior to CHF in a uniformly heated channel.

(3) No change of bulk flow pattern at CHF. Mattson *et al.* [19] describe an experimental fact that there

NOMENCLATURE

c_{pL}	specific heat of liquid at constant pressure
d	i.d. of tube
f	friction factor for homogeneous flow
G	mass velocity
h_{FC}	forced convection heat transfer coefficient
H_{fg}	latent heat of evaporation
i_L	local liquid enthalpy (function of T_L)
i_{sat}	enthalpy of saturated liquid
k	vapor velocity coefficient, equation (8)
L_B	length of vapor blanket
Pr_L	Prandtl number of liquid, $\mu_L c_{pL}/\lambda_L$
q	heat flux
q_c	critical heat flux
q_B	fraction of q for boiling
q_{FC}	fraction of q for forced convection
Re	Reynolds number for homogeneous flow, Gd/μ
T_L	local liquid temperature (function of i_L)
T_{sat}	saturation temperature
T_w	wall temperature
U_B	vapor blanket velocity
U_δ	homogeneous flow velocity at distance δ from wall
x	true quality
x_e	local thermodynamic equilibrium quality, $(i_L - i_{sat})/H_{fg}$
$x_{e,N}$	x_e at the incipience of net vapor generation.

Greek symbols

α	void fraction
δ	sublayer thickness
λ_L	thermal conductivity of liquid
μ	viscosity for homogeneous flow
μ_L	viscosity of liquid
μ_v	viscosity of vapor
ρ	density for homogeneous flow
ρ_L	density of liquid
ρ_v	density of vapor
σ	surface tension
τ	vapor blanket passage time
τ_w	wall shear stress of homogeneous flow.

is no abrupt visible change in the bulk flow pattern at CHF.

(4) Effect of wall thickness. The effect of wall thickness on CHF has long been known, but Del Valle M. [20] confirms it rather systematically for CHF in subcooled flow boiling on a sufficiently thin wall.

Now, it is widely admitted that CHF of subcooled or low quality flow boiling has strong similarities to pool boiling CHF, both in mechanism and in behavior (see Whalley [21]); and in fact, a popular name of DNB (departure from nucleate boiling) has long been used for this type of CHF. If attention is paid to this matter, it seems worth attempting such analyses of CHF for both pool and subcooled flow boiling as based on common physical principles.

On this point, it may be of interest to note that Haramura and Katto [22] have already presented a physical model of saturated pool boiling CHF based on the sublayer dryout mechanism. Basic principles associated with the foregoing model of Fig. 1 are as follows: (1) mean length L_B of vapor slugs blanketing a heated surface is governed by the hydrodynamic instability of the vapor–liquid interface, (2) residence time τ of a vapor slug on the sublayer is dominated by the motion of the slug, and (3) initial thickness δ of a liquid sublayer, determined as a critical length of tiny vapor jets anchored to active sites on the heated wall, is given by the following generalized equation:

$$\frac{\delta \rho_v}{\sigma} \bigg/ \left(\frac{\rho_v H_{fg}}{q}\right)^2 = \frac{\pi (0.0584)^2}{2} \left(\frac{\rho_v}{\rho_L}\right)^{0.4} \left(1 + \frac{\rho_v}{\rho_L}\right). \quad (1)$$

In the present paper, an analysis of subcooled flow boiling CHF will be attempted relying on physical principles similar to the foregoing three basic principles for pool boiling CHF.

2. PHYSICAL MODEL FOR THE ONSET OF CHF

A flow configuration illustrated schematically in Fig. 2 is assumed in the present study to explain the onset of CHF in subcooled flow boiling. Through accumulation and condensation of the vapor furnished from the wall, a thin vapor layer or slug (which is termed 'vapor blanket' below) is formed overlying a very thin liquid sublayer adjacent to the wall, and CHF is assumed to occur when the liquid sublayer of

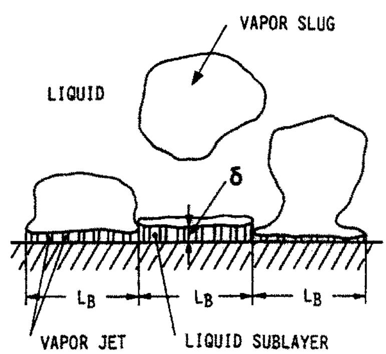

FIG. 1. Saturated pool boiling near CHF conditions.

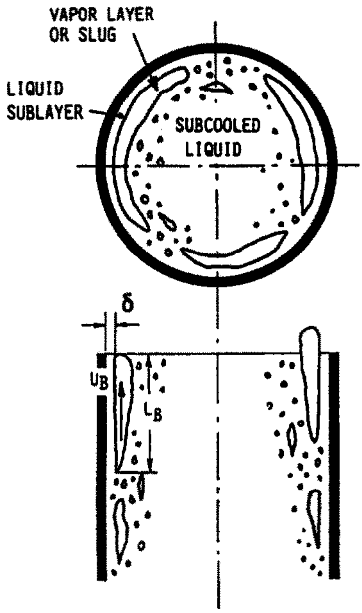

FIG. 2. Subcooled flow boiling near CHF conditions.

initial thickness δ (see the top part of the vapor blanket shown in Fig. 2) is extinguished by evaporation during the passage time of the vapor blanket $\tau = L_B/U_B$, where L_B and U_B are the length and velocity of the vapor blanket, respectively.

2.1. *Initial thickness of liquid sublayer* δ

The liquid sublayer underneath the vapor blanket is generally very thin, so it may be assumed to be in a situation similar to that of Fig. 1: in other words, equation (1) can be used to evaluate δ in principle. However, in the incipient stage of the development of a new vapor blanket near the wall, during which a liquid sublayer is gradually separated from the bulk region, boiling is caused by a fraction q_B of the total heat flux q in the case of subcooled flow boiling. Hence, q in equation (1) is replaced by q_B as

$$\delta = \frac{\pi(0.0584)^2}{2}\left(\frac{\rho_v}{\rho_L}\right)^{0.4}\left(1+\frac{\rho_v}{\rho_L}\right)\frac{\sigma}{\rho_v}\left(\frac{\rho_v H_{fg}}{q_B}\right)^2 \quad (2)$$

with

$$q_B = q - q_{FC} \quad (3)$$

where q_{FC} is the part of the heat flux transferred by forced convection of subcooled liquid. In this paper, q_{FC} will be evaluated relying on the study of Shah [23], who investigated a general correlation for subcooled flow boiling heat transfer of water, refrigerants and organic fluids over a wide range of subcooling $T_{sat} - T_L = 0-153$ K. According to Shah, q_{FC} is written as

$$q_{FC} = h_{FC}(T_w - T_L) \quad (4)$$

where h_{FC} is the single-phase forced-convection heat transfer coefficient given by the well-known Dittus–Boelter equation

$$\frac{h_{FC}d}{\lambda_L} = 0.023\left(\frac{Gd}{\mu_L}\right)^{0.8} Pr_L^{0.4} \quad (5)$$

and $T_w - T_L$, the temperature difference between the wall and liquid, can be predicted by the following equation:

$$T_w - T_L = \frac{(\Psi_0 - 1)(T_{sat} - T_L) + (q/h_{FC})}{\Psi_0} \quad (6)$$

where

$$\Psi_0 = 230(q/GH_{fg})^{0.5}.$$

2.2. *Length of vapor blanket* L_B

As has already been mentioned, the liquid sublayer adjacent to the wall is generally thin so that it can be approximately assumed to rest on the wall, while the vapor blanket flows at a mean velocity U_B (Fig. 2). If it is then postulated that the mean length L_B of vapor blankets is equal to the critical wavelength of Helmholtz instability of the liquid–vapor interface, L_B is readily given as

$$L_B = \frac{2\pi\sigma(\rho_v + \rho_L)}{\rho_v \rho_L U_B^2}. \quad (7)$$

It may be of interest to note that substantially the same procedure as above has already beem employed by Lee and Mudawar [14] to evaluate the vapor blanket length in their CHF model based on the sublayer dryout mechanism.

2.3. *Velocity of vapor blanket*

In the case of subcooled flow boiling, the vapor blanket formed near the wall is comparatively thin because of being subject to condensation by the subcooled core flow. Accordingly, it can be assumed that the moving velocity U_B of the blanket has some close relations to the local velocity of homogeneous two-phase flow U_δ at a distance δ from the wall, and hence

$$U_B = kU_\delta \quad (8)$$

where k is a coefficient, the value of which is presumably less than unity because of the situation that the vapor blanket is maintained through continuous supply of vapor from the stationary wall or the stagnant liquid sublayer. The magnitude of k will be analyzed later in Section 3. The velocity U_δ on the right-hand side equation (8) is evaluated as follows.

2.3.1. *Magnitude of true quality* x. First, according to Saha and Zuber [24], the true quality x of the subcooled two-phase flow in a heated tube can be evaluated by the following equation:

$$x = \frac{x_e - x_{e,N}\exp\left(\dfrac{x_e}{x_{x,N}} - 1\right)}{1 - x_{e,N}\exp\left(\dfrac{x_e}{x_{e,N}} - 1\right)}. \quad (9)$$

In this equation, x_e is the thermodynamic equilibrium quality defined by

$$x_e = \frac{i_L - i_{sat}}{H_{fg}} \tag{10}$$

where i_L is the enthalpy of subcooled liquid at the location where CHF takes place, and i_{sat} the enthalpy of the saturated liquid. Meanwhile, $x_{e,N}$ in equation (9), the thermodynamic equilibrium quality at the location to initiate the net vapor generation downstream of the incipient nucleate boiling point, is evaluated by

$$x_{e,N} = -0.0022 \frac{q}{\rho_L H_{fg}} \frac{d}{(\lambda_L / c_{pL} \rho_L)} \quad \text{for} \quad Pe_L = G c_{pL} d/\lambda_L < 70\,000$$

$$x_{e,N} = -154 \frac{q}{\rho_L H_{fg}} \frac{1}{(G/\rho_L)} \quad \text{for} \quad Pe_L = G c_{pL} d/\lambda_L > 70\,000. \tag{11}$$

For the calculation of equation (11), physical properties of the saturated liquid are used for simplicity in this paper. In addition, equation (9) gives $x = 0$ when $x_e = x_{e,N}$: and it can be assumed further that

$$x = 0, \quad \text{if } x_e \leqslant x_{e,N}. \tag{12}$$

2.3.2. *Magnitude of ρ and μ for homogeneous flow.* For the homogeneous two-phase flow of true quality x, the fluid density ρ is generally given by

$$\frac{1}{\rho} = \frac{x}{\rho_v} + \frac{1-x}{\rho_L} \tag{13}$$

while the viscosity μ will be evaluated in the present paper by the following equation recently presented by Beattie and Whalley [25]:

$$\mu = \mu_v \alpha + \mu_L (1-\alpha)(1+2.5\alpha) \tag{14}$$

where α is the void fraction to be evaluated by

$$\alpha = \frac{x}{x + (1-x)(\rho_v/\rho_L)}. \tag{15}$$

2.3.3. *Magnitude of velocity U_δ.* For the homogeneous turbulent flow in a tube with fluid density ρ and viscosity μ, the velocity U_δ at a distance δ from the wall surface can be evaluated by the Karman velocity distribution as

$$\left.\begin{array}{ll} \text{if} \quad 0 < y_\delta^+ < 5, & U_\delta^+ = y_\delta^+ \\ \text{if} \quad 5 < y_\delta^+ < 30, & U_\delta^+ = 5.0 + 5.0 \ln (y_\delta^+/5) \\ \text{if} \quad 30 < y_\delta^+, & U_\delta^+ = 5.5 + 2.5 \ln y_\delta^+ \end{array}\right\} \tag{16}$$

where

$$\left.\begin{array}{l} y_\delta^+ = \delta \sqrt{(\tau_w/\rho)}/(\mu/\rho) \\ U_\delta^+ = U_\delta / \sqrt{(\tau_w/\rho)}. \end{array}\right\} \tag{17}$$

The magnitude of the wall shear stress τ_w in equation (17) is given by

$$\tau_w = f \cdot \rho \frac{(G/\rho)^2}{8} \tag{18}$$

where the friction factor f can be evaluated through the well-known Prandtl–Karman formula

$$1/\sqrt{f} = 2.0 \log_{10} (Re \sqrt{f}) - 0.8 \tag{19}$$

where Re is the Reynolds number defined by

$$Re = \frac{(G/\rho)d}{(\mu/\rho)} = \frac{Gd}{\mu}. \tag{20}$$

It may be of use to note that the Reynolds number of equation (20) has been checked for all of the existing experimental data of subcooled flow boiling listed in Table 1, revealing an interesting fact that they are entirely in the turbulent flow regime without exception.

2.4. *Critical heat flux*

L_B and U_B given by equations (7) and (8), respectively, determine the passage time of a vapor blanket τ as

$$\tau = L_B / U_B. \tag{21}$$

Then the minimum heat flux q' necessary to extinguish a sublayer of initial thickness δ by evaporation during the period τ, is

$$q' = \delta \rho_L H_{fg} / \tau \tag{22}$$

and q' is equal to the heat flux q, which has been included in equations (3), (6), and (11), when q is the critical heat flux. Thus, for given conditions of tube diameter d, pressure p, mass velocity G, local value of subcooling $T_{sat} - T_L$, and equilibrium quality x_e corresponding to the subcooling, the critical heat flux q can be predicted by an iterative procedure through the foregoing equations (2)–(22).

3. VELOCITY COEFFICIENT k

3.1. *Correlation of velocity coefficient k*

In the foregoing CHF model, the velocity coefficient k in equation (8) is not fixed, its magnitude is presumed to be less than unity and to vary to some extent depending on the two-phase flow conditions. In the present study, therefore, an analysis of k will be attempted based on a total of 374 data points of subcooled flow boiling of water included in the tabular CHF data of the USSR Academy of Sciences [26] (see Table 1).

Three hundred and seventy-four data points of k value thus derived through equations (2)–(22) so as to fit each of the foregoing tabular CHF data, are divided into four groups by void fraction α, and then analyzed carefully leading to the results of Figs. 3 ($\alpha = 0.7$–1.0), 4 ($\alpha = 0.25$–0.7), 5 ($\alpha = 0$–0.25), and 6 ($\alpha = 0$), where $k \cdot Re^{0.8}$ is plotted against the vapor/liquid density ratio ρ_v/ρ_L. A rather systematic change in character will be noticed between these four figures. The mean values of k are 0.16, 0.13, 0.094, and 0.055 for Figs. 3, 4, 5, and 6, respectively, being certainly less than unity as presumed in Section 2.3.

Table 1. Experimental conditions and prediction accuracy for CHF data analyzed

Fluid	No. of data	Data of $\alpha < 0.7$	d (mm)	p (MPa)	G ($\mathrm{kg\,m^{-2}\,s^{-1}}$)	$T_{sat} - T_L$ (K)	$-x_e$	$\mu(R)$	$\sigma(R)$	Ref.
Water	374	306	8	2.9–19.6	500–5000	0–75	0–0.835	1.003	0.190	[26]
Water	290†	263	1.14–11.07	2.1–13.8	350–15 560	1.8–97.6	0.01–0.493	1.068	0.163	[27]
R-12	53‡	53	5	1.9–3.4	770–5400	0.2–10.4	0.004–0.264	1.159	0.247	[28, 29]
R-11	37	37	12.5	1.0–2.5	1390–8800	18.3–61.3	0.155–0.619	1.182	0.247	[30]
Nitrogen	51	51	12.8	0.5–1.7	550–2260	3.0–26.2	0.041–0.477	1.337	0.215	[31]
Helium	11	11	1	0.199	35–90	0–0.159	0.021–0.191	1.614	0.294	[32]
Helium	4	4	1.09	0.194–0.199	78–104	0–0.198	0.034–0.216	1.641	0.337	[33]
R-113	35	35	10.2	0.9–2.2	1280–5600	0.47–30.8	0.005–0.544	1.632	0.411	[34]

† Clearly nine abnormal data points have been omitted from the original data.
‡ Data points of $\Delta p/p > 0.03$ have been omitted from the original data.

The present model based on the assumption of homogeneous flow is of course inapplicable to CHF in annular flow, and annular flow is usually assumed to be bounded near $\alpha = 0.8$. In this paper, therefore, excepting the data of Fig. 3 for $\alpha = 0.7$–1.0, correlations of k are derived from the rest data of Figs. 4–6 as follows:

for $\alpha = 0.25$–0.7

$$k = \frac{6.4 \times 10^3}{1 + 87.3(\rho_v/\rho_L)^{1.28}} Re^{-0.8} \tag{23}$$

for $\alpha = 0$–0.25

$$k = \frac{1.5 \times 10^4}{1 + 87.2(\rho_v/\rho_L)^{1.19}} Re^{-0.8} \tag{24}$$

for $\alpha = 0$

$$k = \frac{6 \times 10^3}{1 + 254(\rho_v/\rho_L)^{2.83}} Re^{-0.8} \tag{25}$$

where α and Re are given by equations (15) and (20), respectively. Of course, it is recommended that the above three equations (23)–(25) be employed within

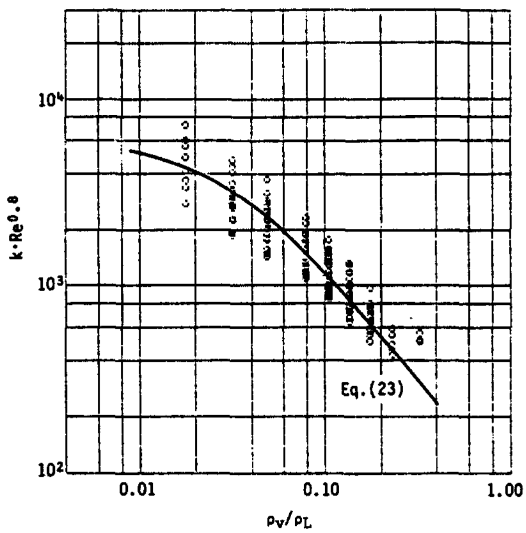

FIG. 4. Velocity coefficient (void fraction: $0.25 \leq \alpha < 0.7$).

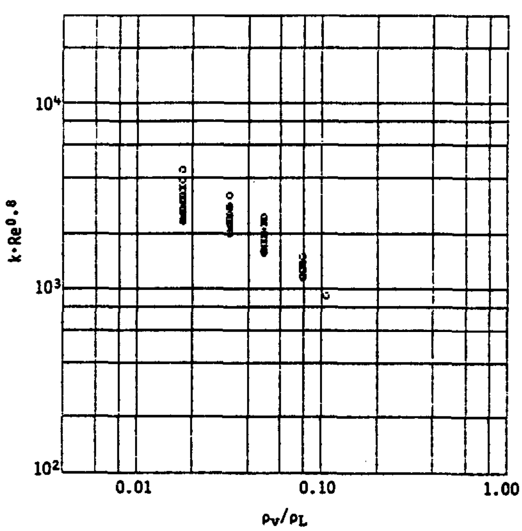

FIG. 3. Velocity coefficient (void fraction: $0.7 \leq \alpha < 1.0$).

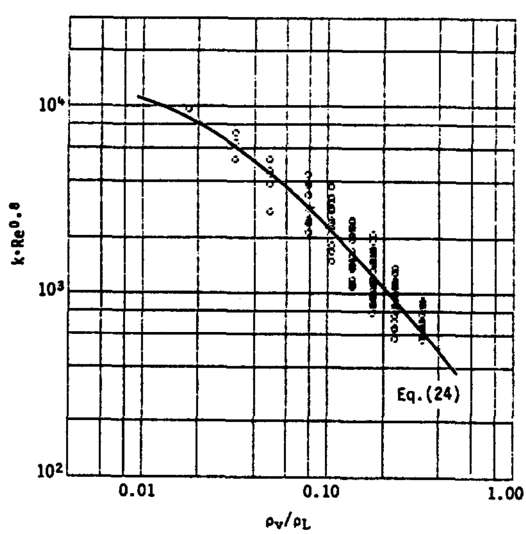

FIG. 5. Velocity coefficient (void fraction: $0 < \alpha < 0.25$).

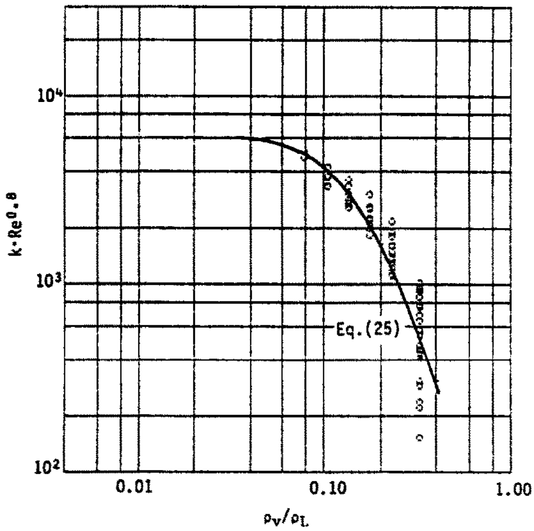

FIG. 6. Velocity coefficient (void fraction: $\alpha = 0$).

the region of vapor/liquid density ratio ρ_v/ρ_L greater than 0.01 (see Figs. 4–6).

3.2. *Predictive procedure of CHF*

In the preceding section, correlations of k were obtained separately for three individual regimes of void fraction α. Hence, if these correlations are employed to predict CHF, an inconsistent situation can appear near the boundary of two adjacent regimes of α: for example, if k of equation (23) for $\alpha > 0.25$ is employed, it predicts CHF at $\alpha < 0.25$, while if k of equation (24) for $\alpha < 0.25$ is employed, it predicts CHF at $\alpha > 0.25$.

However, this problem can be solved by introducing an averaging procedure. Namely, as for the states predicted by equations (2)–(22), let three sets of void fraction α and critical heat flux q_c obtained with k of equations (23), (24), and (25), respectively, be written as (α_1, q_1), (α_2, q_2), and (α_3, q_3). Then, denoting the final value of CHF to be determined from the above three values of q by q_c, the following calculation procedure can be composed.

(a) Start the calculation by employing k of equation (23) for $0.25 < \alpha < 0.7$, which gives α_1 and q_1.

(a-1) If $0.7 \leqslant \alpha_1$, the present model is inapplicable.

(a-2) If $0.25 \leqslant \alpha_1 < 0.7$, put $q_c = q_1$ and stop the calculation.

(a-3) If $\alpha_1 < 0.25$, proceed to the next step (b).

(b) Make the calculation with k of equation (24) for $0 < \alpha < 0.25$, which gives α_2 and q_2.

(b-1) If $0.25 \leqslant \alpha_2$, put $q_c = (q_1+q_2)/2$ and stop the calculation.

(b-2) If $0 < \alpha_2 < 0.25$, put $q_c = q_2$ and stop the calculation.

(b-3) If $\alpha_2 = 0$, proceed to the next step (c).

(c) Make the calculation with k of equation (25) for $\alpha = 0$, which gives α_3 and q_3.

(c-1) If $0 < \alpha_3$, put $q_c = (q_2+q_3)/2$ and stop the calculation.

(c-2) If $\alpha_3 = 0$, put $q_c = q_3$ and stop the calculation.

It may be useful to add here that the same procedure is also applicable to evaluate the magnitude of the quantities such as δ, L_B, and U_B.

3.3. *Accuracy of prediction*

The accuracy of the foregoing predictive procedure is checked for all of the USSR subcooled flow boiling data [26], giving the result of Table 2, where R is defined as

$$R = (\text{predicted } q_c)/(\text{measured } q_c) \tag{26}$$

and $\mu(R)$ and $\sigma(R)$ are the mean value and the standard deviation of R, respectively; INTER-1 and INTER-2 are the intermediate regions where q_c is determined by the foregoing averaging procedure of (b-1) and (c-1), respectively.

It is noticed from Table 1 that the present predictive procedure has good accuracy over the whole range of subcooled conditions in the USSR tabular CHF data. Since the Lee–Mudawar model [14] is based on the sublayer dryout mechanism, its prediction accuracy for the same data groups as above is also shown in Table 2, for reference.

3.4. *Magnitudes of δ, L_B, U_B, and τ*

As for the magnitude of δ (sublayer thickness), L_B (blanket length), U_B (blanket velocity), and τ (blanket passage time) appearing in the present model, the distribution range and mean value of the data obtained in the course of the calculation for Table 2 are listed in Table 3, omitting INTER-1 and INTER-2 regimes for simplicity. Though there are no existing experimental data to be compared with the predicted values of these quantities, it will be noticed that the magnitudes of δ and L_B, for example, seem to be of rather reasonable order judging from a physical sense.

For reference, Table 4 shows the results of the Lee–Mudawar model for the same conditions. As compared with the case of Table 3, the magnitudes of δ, L_B, and τ in Table 4 are excessively small.

4. GENERALITY OF CORRELATION OF VELOCITY COEFFICIENT *k*

The USSR tabular CHF data [26], from which the correlation equations (23)–(25) of k have been derived in Section 3, are restricted to the conditions of tube diameter $d = 8$ mm and water only. However, the foregoing correlation equations are expressed in generalized forms, respectively, so it is of interest to examine their generality by comparing the predicted CHF with the measured value for diameters other than 8 mm as well as for non-aqueous fluids.

Table 2. Prediction accuracy for water data of ref. [26]

	No. of data	Present work $\mu(R)$	Present work $\sigma(R)$	Lee–Mudawar $\mu(R)$	Lee–Mudawar $\sigma(R)$
$0.7 \leqslant \alpha$	68	—	—	—	—
$0.25 \leqslant \alpha < 0.7$	94	1.055	0.199	1.025	0.140
INTER-1	63	1.071	0.124	1.090	0.178
$0 < \alpha < 0.25$	65	0.978	0.199	1.222	0.435
INTER-2	23	0.999	0.092	0.969	0.139
$\alpha = 0$	61	0.945	0.110	1.474	0.569
Total	374				

Table 3. Magnitudes of δ, L_B, U_B, and τ predicted by the present model under conditions of water data [26]

	No. of data	δ (μm) range	δ (μm) mean	L_B (mm) range	L_B (mm) mean	U_B (m s^{-1}) range	U_B (m s^{-1}) mean	τ (ms) range	τ (ms) mean
$0.25 \leqslant \alpha < 0.7$	94	23.0–661	192	3.88–20.2	10.3	0.0625–1.60	0.447	3.24–261	44.6
$0 < \alpha < 0.25$	65	50.9–662	214	3.53–11.0	6.59	0.0813–0.942	0.260	5.62–119	36.5
$\alpha = 0$	61	49.5–953	341	2.35–13.3	5.78	0.0756–0.999	0.242	3.86–147	47.3

Table 4. Magnitudes of δ, L_B, U_B, and τ predicted by the Lee–Mudawar model [14] under the same conditions as Table 3

	No. of data	δ (μm) range	δ (μm) mean	L_B (mm) range	L_B (mm) mean	U_B (m s^{-1}) range	U_B (m s^{-1}) mean	τ (ms) range	τ (ms) mean
$0.25 \leqslant \alpha < 0.7$	94	0.294–40.8	10.9	0.141–4.31	1.61	0.328–3.52	1.19	0.307–9.28	2.36
$0 < \alpha < 0.25$	65	0.008–18.7	3.59	0.003–1.30	0.409	0.346–4.60	1.41	0.0007–3.32	0.557
$\alpha = 0$	61	0.010–6.02	0.926	0.003–1.06	0.127	0.467–4.60	2.08	0.0007–0.927	0.109

4.1. *Effect of diameter on CHF*

Experimental data of CHF obtained for different diameters fixing all other conditions are scarce: three data points plotted in Fig. 7 are those found with some difficulty from the CHF data of water compiled by Thompson and Macbeth [27], being restricted within a very narrow range of pressure $p = 13.79$ MPa, mass velocity $G = 2034 \sim 2101$ kg m^{-2} s^{-1}, and equilibrium quality $x_e = -0.142 \sim -0.149$. Meanwhile, thin lines in Fig. 7 represent the predicted variation of CHF with diameter for the condition of $p = 13.79$ MPa, $G = 2065$ kg m^{-2} s^{-1}, and $x_e = -0.146$; and its average trend is indicated by a thick line. It can be noticed in Fig. 7 that the predicted CHF agrees fairly well, not only with the three data points mentioned above, but also with the empirical rule of $q_c \propto (1/d)^{1/2}$ recommended in connection with the USSR tabular data for $d = 0.8$ mm [26]. In addition, Fig. 7 shows an interesting fact that the void fraction α (or the true quality x) at CHF conditions

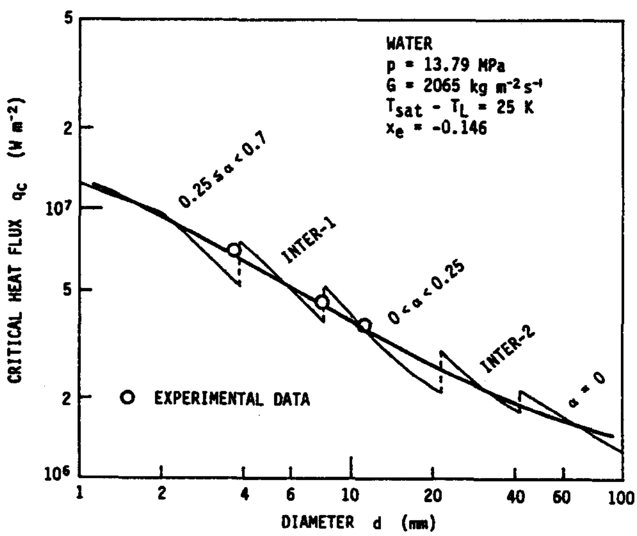

FIG. 7. Variation of critical heat flux with tube diameter.

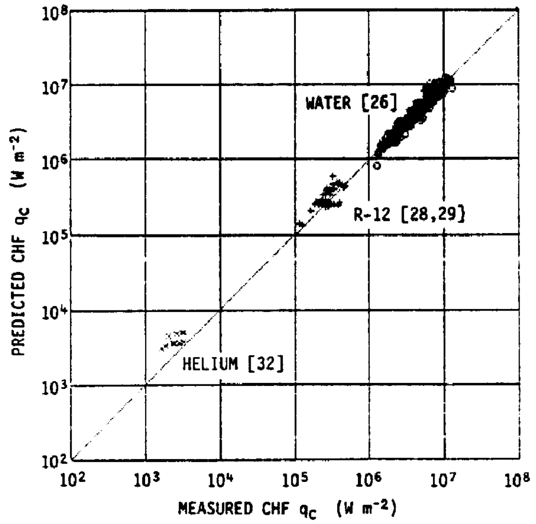

FIG. 8. Comparison of predicted and measured critical heat flux.

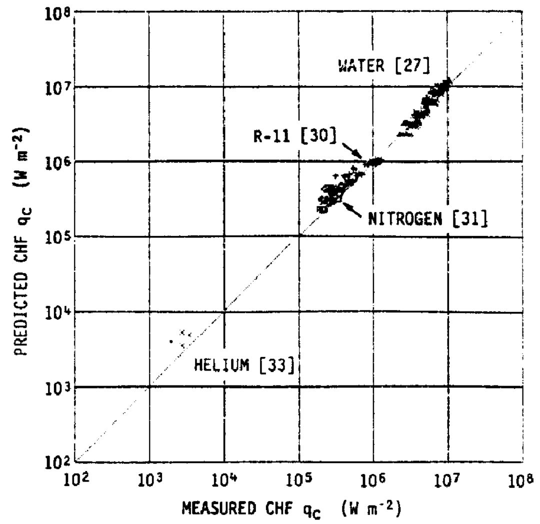

FIG. 9. Comparison of predicted and measured critical heat flux.

varies noticeably with the change of tube diameter even though equilibrium quality x_e is fixed.

For a further check of the applicability of the present predictive procedure to diameters other than 8 mm, the predicted CHF values are also compared with 290 data points of subcooled flow boiling included in the foregoing Thompson–Macbeth compilation [27]. The results of $\mu(R)$ and $\sigma(R)$ in this case are shown on the second column of Table 1 along with the extent of diameter, indicating good accuracy similar to that for the USSR tabular data [26] shown on the first column of the same table.

4.2. *CHF of non-aqueous fluids*

Next, the predicted values of CHF will be compared with the experimental data of subcooled flow boiling obtained for R-12 by Katto and co-workers [28, 29], R-11 by Purcupile *et al.* [30], liquid nitrogen by Papell *et al.* [31], liquid helium by Katto and Yokoya [32], liquid helium by Ogata and Sato [33], and R-113 by Coffield *et al.* [34], respectively. Among the above, the data of R-12 are those based on the inlet pressure of the uniformly heated tube, accordingly such data with pressure drop Δp through the heated tube as high as $\Delta p/p > 0.03$ have been excluded in the present paper to assure correct values of physical properties at the tube exit end where CHF occurred.

In Figs. 8–10, comparisons of the predicted values of CHF with the data of non-aqueous fluids are presented, together with comparisons with the data of water of the USSR Academy of Sciences (Fig. 8) and those of Thompson–Macbeth (Fig. 9); and $\mu(R)$ and $\sigma(R)$ for each case are presented in Table 1. It may be concluded from these results that the present model is useful to predict CHF for water over a wide range of subcooling as shown in Table 1, and at the same time, is applicable to predict CHF for non-aqueous fluids if one only is prepared for a certain measure of

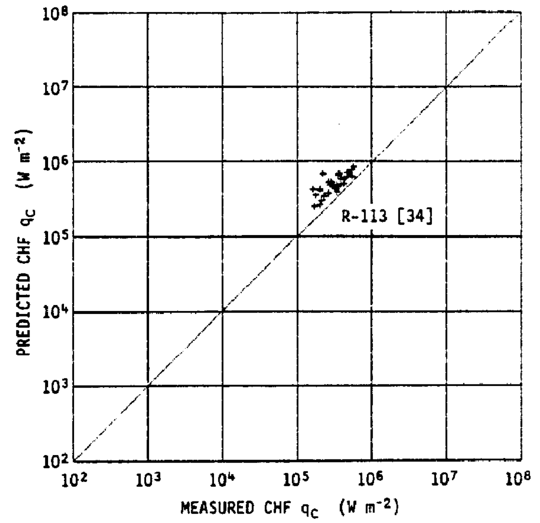

FIG. 10. Comparison of predicted and measured critical heat flux.

reduction of accuracy to some fluids. Anyhow, this result for non-aqueous fluids may be regarded as astounding if it is recalled that the present model has been developed with a very simple framework.

5. CONCLUSIONS

A physical approach has been attempted to CHF of subcooled flow boiling in tubes based on the liquid sublayer dryout mechanism. The sublayer thickness is evaluated by the same equation as that derived in a previous analysis of CHF in pool boiling [22]; and the length and velocity of a vapor blanket sliding on the sublayer are then estimated on the assumptions of Helmholtz instability and homogeneous flow, respectively. A coefficient, that is introduced to connect the blanket velocity with the homogeneous flow velocity, is correlated empirically as a function of Reynolds number and vapor/liquid density ratio relying on the USSR tabular CHF data [26]. A problem, which arises from the discrete correlations of the foregoing coefficient in three finite regimes of void fraction, is solved by employing an averaging procedure near the boundary of two adjacent regimes of void fraction. The CHF model thus developed can predict CHF of water with good accuracy over a wide range of subcooling, and besides, an interesting fact has been found that the void fraction at CHF conditions varies with the change of tube diameter under a fixed condition of equilibrium quality. Finally, if one only permits a measure of reduction of accuracy to some fluids, this model is capable of being used for approximate predictions of CHF of non-aqueous fluids.

REFERENCES

1. L. S. Tong, H. B. Currin, P. S. Larsen and O. G. Smith, Influence of axially nonuniform heat flux on DNB, *Chem. Engng Prog. Symp. Ser.* **62**(64), 35–40 (1965).
2. S. S. Kutateladze and A. I. Leont'ev, Some applications of the asymptotic theory of the turbulent boundary layer, *Proc. 3rd Int. Heat Transfer Conf.*, Vol. III, pp. 1–6 (1966).
3. L. S. Tong, Boundary layer analysis of the flow boiling crisis, *Int. J. Heat Mass Transfer* **11**, 1208–1211 (1968).
4. L. S. Tong, A phenomenological study of critical heat flux, ASME Paper 75-HT-68 (1975).
5. J. C. Purcupile and S. W. Gouse, Jr., Reynolds flux model of critical heat flux in subcooled forced convection boiling, ASME Paper 72-HT-4 (1972).
6. W. T. Hancox and W. B. Nicoll, On the dependence of the flow-boiling heat transfer crisis on local near-wall conditions, ASME Paper 73-HT-38 (1973).
7. E. J. Thorgerson, D. H. Knoebel and J. H. Gibbons, A model to predict convective subcooled critical heat flux, *Trans. ASME*, Series C, *J. Heat Transfer* **96**, 79–82 (1974).
8. B. R. Bergel'son. Burnout under conditions of subcooled boiling and forced convection, *Thermal Engng* **27**(1), 48–50 (1980).
9. I. P. Smogalev, Calculation of critical heat fluxes with flow of subcooled water at low velocity, *Thermal Engng* **28**(4), 208–211 (1981).
10. W. Hebel, W. Detavernier and M. Decreton, A contribution to the hydrodynamics of boiling crisis in a forced flow of water, *Nucl. Engng Des.* **64**, 433–445 (1981).
11. J. Weisman and B. S. Pei, Prediction of critical heat flux in flow boiling at low qualities, *Int. J. Heat Mass Transfer* **26**, 1463–1477 (1983).
12. J. Weisman and S. H. Ying, Theoretically based CHF prediction at low qualities and intermediate flows, *Trans. Am. Nucl. Soc.* **45**, 832–833 (1983).
13. V. V. Yagov and V. A. Puzin, Burnout under conditions of forced flow of subcooled liquid, *Thermal Engng* **32**(10), 569–572 (1985).
14. C. H. Lee and I. Mudawar, A mechanistic critical heat flux model for subcooled flow boiling based on local bulk flow conditions, *Int. J. Multiphase Flow* **14**, 711–728 (1988).
15. L. S. Tong, L. E. Effering and A. A. Bishop, A photographic study of subcooled boiling flow and DNB of Freon-113 in a vertical channel, ASME Paper 66-WA/HT-39 (1966).
16. M. P. Fiori and A. E. Bergles, Model of critical heat flux in subcooled flow boiling, *Proc. 4th Int. Heat Transfer Conf.*, Vol. VI, p. B6.3 (1970).
17. S. B. van der Molen and F. W. B. M. Galjee, The boiling mechanism during burnout phenomena in subcooled two-phase water flows, *Proc. 6th Int. Heat Transfer Conf.*, Vol. 1, pp. 381–385 (1978).
18. R. Hino and T. Ueda, Studies on heat transfer and flow characteristics in subcooled flow boiling—Part 2. Flow characteristics, *Int. J. Multiphase Flow* **11**, 283–298 (1985).
19. R. J. Mattson, F. G. Hammitt and L. S. Tong, A photographic study of the subcooled flow boiling crisis in Freon-113, ASME Paper 73-HT-39 (1973).
20. V. H. Del Valle M., An experimental study of critical heat flux in subcooled flow boiling at low pressure including the effect of wall thickness, *ASME–JSME Thermal Engng Joint Conf. Proc.*, Vol. 1, pp. 143–150 (1983).
21. P. B. Whalley, *Boiling, Condensation, and Gas–Liquid Flow*, p. 155. Clarendon Press, Oxford (1987).
22. Y. Haramura and Y. Katto, A new hydrodynamic model of critical heat flux, applicable widely to both pool and forced convection boiling on submerged bodies in saturated liquids, *Int. J. Heat Mass Transfer* **26**, 389–399 (1983).
23. M. M. Shah, A general correlation for heat transfer during subcooled boiling in pipes and annuli, *ASHRAE Trans.* **83**, 202–217 (1977).
24. P. Saha and N. Zuber, Point of net vapor generation and vapor void fraction in subcooled boiling, *Proc. 5th Int. Heat Transfer Conf.*, Vol. IV, pp. 175–179 (1974).
25. D. R. H. Beattie and P. B. Whalley, A simple two-phase frictional pressure drop calculation method, *Int. J. Multiphase Flow* **8**, 83–87 (1982).
26. Heat Mass Transfer Section, Scientific Council, Academy of Sciences, USSR, Tabular data for calculating burnout when boiling water in uniformly heated round tubes, *Thermal Engng* **23**(9), 77–79 (1972).
27. B. Thompson and R. V. Macbeth, Boiling water heat transfer burnout in uniformly heated round tubes: a compilation of world data with accurate correlations, U.K.A.E.A., AEEW-R356 (1964).
28. Y. Katto and S. Yokoya, CHF of forced convection boiling in uniformly heated vertical tubes: experimental study of HP-regime by the use of refrigerant 12, *Int. J. Multiphase Flow* **8**, 165–181 (1982).
29. Y. Katto and S. Ashida, CHF in high-pressure regime for forced convection boiling in uniformly heated vertical tubes of low length-to-diameter ratio, *Proc. 7th Int. Heat Transfer Conf.*, Vol. 4, pp. 291–296 (1982).
30. J. C. Purcupile, L. S. Tong and S. W. Gouse, Jr., Refrigerant–water scaling of critical heat flux in round tubes—subcooled forced-convection boiling, *Trans. ASME*, Series C, *J. Heat Transfer* **95**, 279–281 (1973).
31. S. S. Papell, R. J. Simoneau and D. D. Brown, Buoyancy effects on critical heat flux of forced convective boiling in vertical flow, NASA, TN D-3672 (1966).
32. Y. Katto and S. Yokoya, Critical heat flux of liquid helium (I) in forced convective boiling, *Int. J. Multiphase Flow* **10**, 401–413 (1984).
33. H. Ogata and S. Sato, Critical heat flux for two-phase flow of helium I, *Cryogenics* **13**, 610–611 (1976).
34. R. D. Coffield, Jr., W. H. Rohrer, Jr. and L. S. Tong, A subcooled DNB investigation of Freon-113 and its similarity to subcooled water DNB data, *Nucl. Engng Des.* **11**, 143–153 (1969).

UNE APPROCHE PHYSIQUE DU FLUX THERMIQUE CRITIQUE DE L'EBULLITION AVEC ECOULEMENT SOUS-REFROIDI DANS LES TUBES CIRCULAIRES

Résumé—On présente une analyse du flux thermique critique (CHF) d'ébullition avec écoulement sous-refroidi, à partir du mécanisme d'assèchement de la sous-couche liquide, en supposant que c'est le même phénomène que le CHF en réservoir à l'exception de différences entre convection forcée et convection naturelle. En employant la même formule d'épaisseur de sous-couche que celle dérivée pour le CHF d'ébullition en réservoir, un modèle physique de CHF est obtenu avec un coefficient empirique relié à la vitesse d'une couche de vapeur glissant sur la mince couche liquide. Des valeurs de CHF prédites sont comparées à des données expérimentales pour eau, R-12, R-11, azote, hélium, et R-113, ce qui suggère la convenance du présent modèle.

EINE PHYSIKALISCHE BETRACHTUNG DER KRITISCHEN WÄRMESTROMDICHTE BEIM UNTERKÜHLTEN STRÖMUNGSSIEDEN IN KREISRUNDEN ROHREN

Zusammenfassung—Diese Arbeit stellt eine analytische Betrachtung der kritischen Wärmestromdichte beim unterkühlten Strömungssieden vor. Als Grundlage dient der Mechanismus des Austrocknens der flüssigen Unterschicht. Es wird angenommen, daß das Phänomen ähnlich dem der kritischen Wärmestromdichte beim Behältersieden ist—abgesehen von offensichtlichen Unterschieden zwischen erzwungener und natürlicher Konvektion. Durch Verwendung derselben Gleichung für die Grenzschichtdicke, die für die kritische Wärmestromdichte beim Behältersieden abgeleitet wurde, ergibt sich ein physikalisches Modell mit einem empirischen Korffizienten für die Geschwindigkeit der über die dünne Flüssigkeitsunterschicht gleitenden Dampfstreifen. Berechnete Werte der kritischen Wärmestromdichte werden mit entsprechenden experimentellen Daten für Wasser, R-12, R-11, Stickstoff, Helium und R-113 verglichen, wobei sich die Gültigkeit des vorgestellten Modells zeigt.

ФИЗИЧЕСКИЙ ПОДХОД К ОПРЕДЕЛЕНИЮ КРИТИЧЕСКОГО ТЕПЛОВОГО ПОТОКА ПРИ КИПЕНИИ НЕДОГРЕТОЙ ЖИДКОСТИ, ДВИЖУЩЕЙСЯ В КРУГЛОЙ ТРУБЕ

Аннотация—На основе механизма осушения жидкого подслоя анализируется критический тепловой поток (КТП) при кипении движущейся недогретой жидкости. Предполагается, что данное явление сходно с кризисом кипения в большом объеме с учетом различий между вынужденной и естественной конвекцией. Исходя из формулы толщины подслоя, выведенной для КТП при кипении в большом объеме, получена физическая модель КТП с эмпирическим коэффициентом, относящимся к скорости скольжения паровой оболочки по тонкому подслою жидкости. Рассчитанные значения КТП сравниваются с экспериментальными данными для воды, R-12, R-11, азота, гелия и R-113.